A composite flow law for wet polycrystalline halite to capture the transition from dislocation creep to solution-precipitation creep

N. Muhammad[1], J.H.P. de Bresser[2], C.J. Peach[2], C.J. Spiers[2]*

[11]Center for Advanced Studies in Physics, GC University Lahore, Pakistan; [2]Experimental Rock Deformation Laboratory, Department of Earth Sciences, Utrecht University, the Netherlands

** nawazmuhammad@gcu.edu.pk*

ABSTRACT: For wet or dry polycrystalline halite, the creep behaviour observed in laboratory experiments at relatively high temperatures and strain rates is generally considered to be controlled by dislocation mechanisms. For fine grained wet materials at low temperature and strain rates, solution-precipitation creep is suggested to dominate. We studied if the transition between these mechanisms can be observed in laboratory experiments, and if so, at what strain rate. We used synthetic and natural wet polycrystalline halite (starting grain sizes ~0.3 and ~4.0 mm, respectively), and deformed these in multiple strain rate step experiments at *in situ* PT conditions of 50 MPa and 125 °C. We also applied the stress relaxation technique, to achieve strain rates approaching 10^{-9} s^{-1}. For higher stresses and strain rates, we found a power law stress exponent *n~11*, while towards lower stress and strain rate, the *n*-value decreased to ~1. This transition took place over the strain rate interval 10^{-8}-10^{-9} s^{-1}. We interpret this behaviour as a transition from glide-controlled dislocation creep at high *n* to solution-precipitation creep at *n*~1, made possible by grain size adjustment through fluid-assisted dynamic recrystallization. We defined a first-order creep law combining a power law and a solution-precipitation law to cover the transition.

1 Introduction

The mechanical behaviour of halite has been studied extensively before in the laboratory; both for dry (<10 ppm by weight) and wet (>10 ppm by weight) conditions, at different temperatures and pressures (Heard 1972; Heard & Ryerson 1986; Wawersik & Zeuch 1986; Spiers et al. 1990; Senseny et al. 1992; Peach et al. 2001; Ter Heege et al. 2005a). For dry conditions, Carter & Hansen (1983), suggested dislocation climb process as rate controlling mechanism, Franssen (1994) concluded that at laboratory strain rates and relatively low temperatures, 250-450 °C, the behaviour is best explained by climb-controlled dislocation creep with climb itself being governed by diffusion through dislocation cores, while at higher temperatures, 500-780 °C, lattice diffusion-controlled creep is dominant. Muhammad (2015) performed pressure stepping tests to investigate the creep behaviour of dry halite in the temperature range 22-350 °C, where a transition was observed from glide to dislocation climb. For wet conditions, several authors have suggested that under laboratory conditions of temperature 23-500 °C, dislocation creep is the main mechanism controlling creep (Heard 1972; Heard & Ryerson 1986; Carter et al. 1993) while other authors concluded that if grain size is small and temperature is low, solution-precipitation creep plays an important role (Spiers et al. 1990; Urai et al. 1986). Ter Heege et al. (2005b) argued based on an experimental study that in wet polycrystalline halite, both dislocation and solution-precipitation mechanisms might contribute to the overall deformation, provided that microstructural modification processes such as dynamic recrystallization and grain growth can take place freely.

Salt rocks in nature are wet rather than dry (Roedder & Bassett 1981; Urai 1983). The creep of these salt rocks usually occurs at strain rates in the range of 10^{-8} to 10^{-15} s^{-1} (Heard 1972; Van Eekelen 1981; Jackson & Talbot 1986). To fully understand the creep behaviour of halite under natural conditions, it thus is of importance to not only know, in general, which mechanisms may control creep of halite, i.e. dislocation vs. solution-precipitation mechanisms, but also to be able to constrain the strain rates under which a given mechanism prevails. The

strain rates relevant for *in situ* deformation, 10^{-8} to 10^{-15} s^{-1}, are difficult to achieve in laboratory experiments. However, one way of approaching such slow strain rates is to perform stress-relaxation experiments (Rutter & Mainprice 1978). In this technique, strain rates as slow as 10^{-9} s^{-1} can be achieved by allowing the stress on a sample to relax through plastic deformation. The experiments are time consuming but result in valuable data regarding creep behaviour at low stresses and slow strain rates.

2 Method

2.1 Sample preparation

In this study, synthetic as well as natural salt samples were used. All samples were manufactured such that they became cylindrical with length in the range of 80-85 mm and diameter 35-36 mm. The synthetic rock salt sample (halite1) was prepared in the laboratory starting from analytical grade NaCl powder from Merck, with an average particle size of 200-400 µm. The powder salt was cold pressed in a hardened steel, piston-cylinder assembly. The powder was axially pressed at 200 MPa for 20 minutes. The resulting cylindrical sample was sealed in a Viton rubber sleeve and was put in a silicone oil pressure vessel for annealing under 100 MPa confining pressure and a temperature of 150 °C for one week. The sample thus obtained had a theoretical density (mass to volume ratio) of 99.5%. For more details about the sample preparation technique, see (Peach 1991). Two natural halite samples (halite2 and 3) were prepared from 'Speisesalz' cores. These cores came from the Asse mine, Germany, and were taken from the ~800 m gallery level and from a depth of > 3 m inside the horizontal gallery wall (Peach 1991, Urai et al. 1987). The samples had a grain size in the range of 3-10 mm. The constituents of the cores were mainly halite (> 98%), a small amount of poly-halite ($K_2SO_4.MgSO_4.2CaSO_4.2H_2O$; ~1%), and some minor quantity of anhydrite. To create a deliquescence condition in our samples, comparable to that at *in-situ,* all samples were moisturized with water < 0.5 wt.% using atomizer in a chamber and carefully measured for its mass increase. These samples were further sealed in 1.0 mm thick polymer "ethylene propylene diene monomer (EPDM)" jackets to avoid contamination of the samples by the confining medium (silicone oil) used in the deformation apparatus.

2.2 Deformation apparatus

The apparatus used for this study was the so-called "Shuttle Vessel" of the experimental rock deformation (HPT) laboratory at the department of Earth Sciences at Utrecht University, also used in a second study of us in this volume The Shuttle Vessel machine is an internally heated 100 MPa confining pressure vessel mounted on a standard 100 kN Instron 1362 loading frame with an electro-mechanical servo-controlled positioning system. The machine is provided with a (Instron standard, +/-50 mm) linear variable differential transformer (LVDT), but to come to an accurate measurement of the sample deformation, a second LVDT (0-25 mm range, H.F. Jensen, Denmark) was installed at the top of the vessel and near the sample. This was done to reduce the effect of the elastic distortion of the apparatus and measure accurately the shortening of the sample, especially during stress relaxation, where very limited natural strain in the order of 0.001 is to be monitored. The temperature was measured by thermocouples at two locations inside the vessel; one was positioned close to the middle of sample and, the other was at the top of the sample. K-type thermocouples were used, which are accurate within ±1 °C. The confining pressure was created by using silicone oil which is kept at constant pressure within ±0.1 MPa using a servo pump. Measurement of the pressure was done using a diaphragm pressure transducer (Teledyne 2403, 100 MPa range). The triaxial apparatus used is very sensitive to the environmental conditions. Therefore, it was carefully calibrated for the effect of pressure and temperature on the load cell.

2.3 Experiments

In total three multistep experiments were performed; one on synthetic (halite1) and two on natural (halite2 and 3) samples. A typical experiment consisted of a few steps at constant strain rate, in the range 5×10^{-5} to 5×10^{-8} s^{-1}. During the constant strain rate part of the test, the sample was deformed until a steady (or near steady) state of stress was reached. Then the piston was arrested and the stress on the sample was allowed to relax until the diminishing force on the sample reached the limits of the load cell resolution. The duration of each relaxation step was a few days.

The synthetic sample, halite1, was deformed by a 3-step repetitive strain rate of 5×10^{-7} s^{-1}, for a natural strain of 0.01-0.03 per step and each step was followed by stress relaxation. The natural samples, halite2 and 3, were tested in a seven strain rate steps (5×10^{-5}, 5×10^{-6}, 5×10^{-7}, 5×10^{-8}, 5×10^{-7}, 5×10^{-6}, 5×10^{-5} s^{-1}), and the relaxation was followed the constant strain rate parts of 5×10^{-6}, 5×10^{-8} and 5×10^{-6} s^{-1}. The experiments were performed at 125 °C sample temperature and 50 MPa confining pressure (a value where dilatancy/microcracking is suppressed, Peach 1991).

2.4 Data acquisition and processing

The data containing pressure, temperature, load, and position (LVDT_1 and 2) were logged throughout the test. The stress on the sample was calculated from the load values by assuming constant volume deformation, correcting the instantaneous change in area value for progressive change in length of the sample. The cumulative strain (shortening) of the sample was calculated as the natural strain, i.e. the natural logarithm of the ratio of the final length and the initial length (shortening taken as positive). The data acquired during stress relaxation was analysed with a dedicated code to produce the plastic strain rate of the sample.

The stress relaxation technique is based on the following. During deformation at constant rate (imposed by a moving piston), some energy gets stored inside the material as elastically stored energy. During relaxation, when the loading piston is arrested, this energy is dissipated through plastic deformation of the sample. Additionally, the elastically stored energy inside the active part (under force) of the machine also dissipates through the plastic strain of the sample, so the data also need to be corrected for the stiffness of machine. To calculate the sample straining, we take the simple assumption that the stress is proportional to strain, provided that other physical conditions (confining pressure, temperature, microstructure) are constant (Rutter & Mainprice 1978). The strain rate at any instant will then be proportional to the stress relaxation rate, with the elastic (Young's) modulus of sample as a constant of proportionality.

The measured total displacement "x_{total}" (from LVDT_2) can be written as the sum of the sample deformation (elastic + plastic) and elastic distortion of apparatus

$$x_{total} = x_{sample} + x_{apparatus} \tag{1}$$

After differentiating time and normalizing this equation using the instantaneous length of the sample, the following relation of plastic strain rate of the sample is obtained:

$$\dot{\varepsilon}_{plastic} = \dot{\varepsilon}_{total} - \frac{1}{E_{sample}}\left(\dot{\sigma}_{sample}\right) - \frac{1}{L_t} S \left(\frac{\partial F}{\partial t}\right) \tag{2}$$

where,

$\dot{\varepsilon}_{plastic}$ = plastic strain rate of sample [s^{-1}]
$\dot{\varepsilon}_{total}$ = total strain rate measured by LVDT_2 [s^{-1}]
E_{sample} = Young's modulus of sample [MPa]
$\dot{\sigma}_{sample}$ = sample stress relaxation rate [$MPas^{-1}$]
L_t = instantaneous length of sample [m]
S = machine stiffness correction constant [mN^{-1}]
$\left(\frac{\partial F}{\partial t}\right)$ = rate of change of force [Ns^{-1}]

3 Results

3.1 Stress vs natural strain and time

The synthetic salt sample, halite1, was deformed in three steps using a similar strain rate of 5×10^{-7} s^{-1}. In each step, the sample was deformed through a very limited amount of natural strain of 0.015-0.02. The stress-strain curve of Figure 1a shows that steady state was not reached in any of the three steps, but the strain hardening rate appears to decrease with increasing strain.

The natural salt samples, halite2 and 3 were deformed in 7-steps (see Table 1 for details), adding 0.025-0.03 strain at each step. The strength of the natural halite samples is almost twice that of the synthetic salt, at strain rate 5×10^{-7} s^{-1}. Steady state was not reached in any of the strain rate steps. The rate of strain hardening differed depending on the strain rate and appeared higher at the higher rates. For the slowest deformation step, 5×10^{-8} s^{-1}, a few stick slip events, due to high friction between deformation piston and seal, were also observed, as seen by the irregular nature of the stress-strain curve.

Although the hardening rate per individual step in strain rate could be established, for both the synthetic and the natural samples, the data were insufficient to uncover a robust trend in changing hardening rate when going from one strain rate to the other. This hampered reliable extrapolation to higher strain, preventing a comparison of differential stress as a function of strain rate at the same strain. Thus, in Table 1, only the values of the differential stress at the end of each step are given.

Table 1: Mechanical data

Sample	$\dot{\varepsilon}$ [s^{-1}]	ε_a	σ [MPa]
Halite1	5×10^{-7}	0.01	7.7
	5×10^{-7}	0.03	8.7
	5×10^{-7}	0.05	9.2
	5×10^{-5}	0.04	22.6
	5×10^{-6}	0.07	21.9
	5×10^{-7}	0.11	16.0
Halite2	5×10^{-8}	0.13	13.1
	5×10^{-7}	0.15	15.7
	5×10^{-6}	0.17	20.3
	5×10^{-5}	0.21	21.1
	5×10^{-5}	0.04	21.8
	5×10^{-6}	0.07	20.9
	5×10^{-7}	0.10	15.3
Halite3	5×10^{-8}	0.13	11.9
	5×10^{-7}	0.16	15.2
	5×10^{-6}	0.18	19.5
	5×10^{-5}	0.22	21.9

$\dot{\varepsilon}$ is the deformation strain rate
ε_a is the natural axial strain at the end of the particular step
σ is the differential stress value at the end of the deformation step

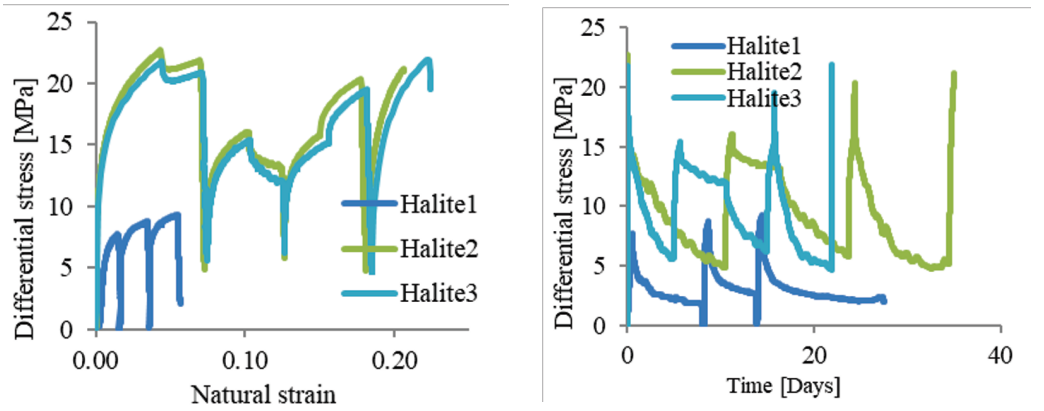

(a) (b)

Figure 1: Strain rate stepping deformation of halite samples showing differential stress against a) natural strain and b) time

3.2 *n*-value for natural halite

The dependence of the differential stress on the strain rate for the natural halite samples (Fig. 2) was tested by applying a conventional power law creep of the type $\dot{\varepsilon} = A\sigma^n$, where $\dot{\varepsilon}$ is the strain rate, σ is the flow stress, and A and n are constants. Since both halite2 and 3 presented substantial strain hardening, any estimate of the constants A and n can only give a first-order impression of the creep behaviour of the material. The data were divided into two parts, for both halite2 and 3; step1 to step4 (decreasing strain rate) and step4 to step7 (increasing strain rate). Linear regression analysis in log-log space resulted in high *n*-values, ranging 10.8-13.6 (Figs. 2(a-b)). Note that the strain rate is the independent variable, but it is shown as dependent in the Figure 2 (i.e. on Y-axis) to compare with the stress relaxation curves (Figs. 3(a-c)).

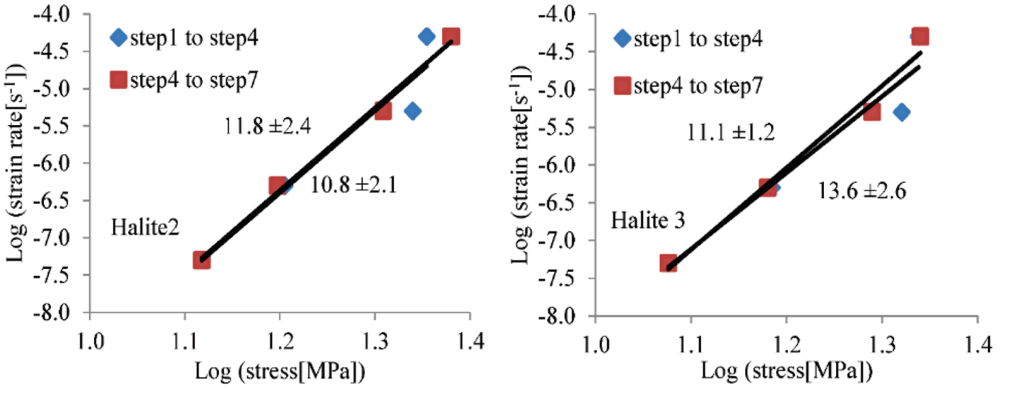

(a) (b)

Figure 2: Log-log plot of strain rate vs. differential stress using the maximum differential stress values at the end of each step. Best fit lines to the data of **a)** halite2 and **b)** halite3, represent power law fits, with corresponding *n*-values indicated.

3.3 Stress relaxation

The stick slip events between deformation piston and seal were more conspicuous during stress relaxation than during deformation. Such events caused great noise in the signal of the measured displacement and, hence, resulted in substantial scatter in calculated strain rate, so the mode values were used instead. Moreover, the relaxation behaviour of all samples appeared identical and we have selected only three as representatives. These are plotted in Figures 3(a-c). The steady state/maximum stress values obtained at the end of each strain rate deformation steps are marked in the graphs along with the projected slopes representing

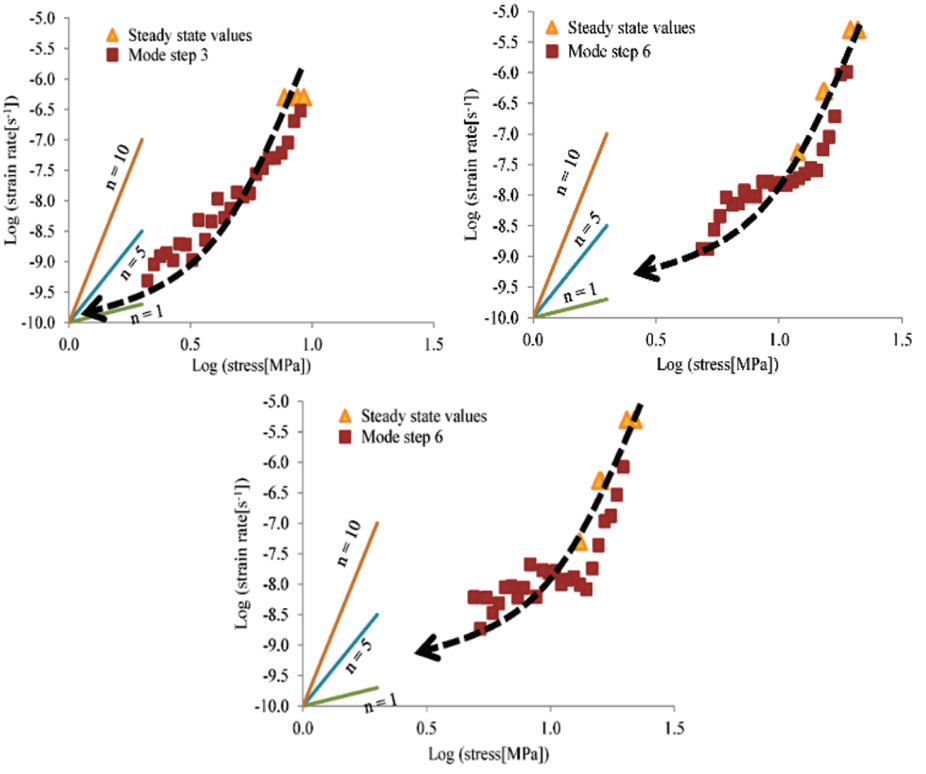

Figure 3: Log-log plot of strain rate vs. differential stress including the results of stress relaxation steps. Closed triangles are the steady state/maximum differential stress values obtained at the end of each step, closed squares are the mode values of the calculated strain rate data. Three slopes representing the *n*-values of 1, 5 and 10 are included to be compared with the trend during relaxation, represented by the free-hand drawn dashed line. Top left: halite1, Top right: halite2, Bottom: halite3

the stress exponent *n*-values (n = 1, 5 and 10) according to scale. Generally, the graphs show that the calculated plastic strain rate at the start of each relaxation period fits to a trend with high *n*-value (>10), implying that the stress is not very sensitive to strain rate. Progressively, the sensitivity increases and the corresponding *n*-value approaches n = 1 for lower stress and slow strain rate values near end of each relaxation step. A free hand dashed-line drawing, showing trend of relaxation is also plotted along to show the expected trend during relaxation.

4 Discussion

The aim of this study was to investigate if a transition can be observed from creep behaviour of halite governed by dislocation mechanisms to creep behaviour controlled by a solution-

precipitation mechanism, and if so, what the conditions of this transition are in terms of strain rate. Below, we will discuss our observations and compare the strength of the halite and its change with decreasing strain rate with the mechanical behaviour established in other studies.

4.1 *n*-value

Fitting the stress-strain rate data obtained during the constant strain rate parts of the multi-step experiments to a conventional power law creep of the type $\dot{\varepsilon} = A\sigma^n$ resulted in a value for *n* larger than 10. Although steady state was not fully reached during the steps, the decrease in strain hardening rate is such that the high *n* values are likely to remain robust at higher strains. Microphysical models for creep controlled by dislocation climb generally result in power law creep equations (Muhammad 2015), but the values for *n* usually range 3-4.5 for climb controlled by lattice diffusion, or up to 6.5 in case of climb controlled by dislocation core (pipe) diffusion (Franssen 1994; Carter et al. 1993; Urai et al. 1987). The value of $n > 10$ appears to rule out climb control for the creep behaviour of wet polycrystalline halite for the conditions tested. Rather, a glide or cross-slip controlled creep model may apply (Spiers et al. 1986). Muhammad (2015) presented results on dry rock salt and showed a low sensitivity of the stress on the strain rate like the wet halite reported here, at comparable conditions of temperature and pressure, at 125 °C and 50 MPa. For the dry halite, it was concluded that a glide mechanism (Weertman 1957; Poirier 1985) rather than a cross slip mechanism (Auten et al. 1973; Skrotzki et al. 1981) controls flow at the given conditions. We infer that the conclusion regarding glide control also holds for the current wet halite.

The stress relaxation behaviour of the wet halite (Figs. 3(a-c)) shows that the *n*-value gradually decreases with decreasing stress and strain rate, reaching ~1 at strain rates below 10^{-8} s^{-1}. This trend is observed in both synthetic and natural halite samples. This strongly suggests that a transition takes place towards grain size sensitive (GSS) creep (Spiers et al. 1990; Ter Heege et al. 2005a; Ding et al. 2021).

If we compare our work with previous studies on halite by using their flow laws (Heard 1972; Wawersik & Zeuch 1986; Ter Heege et al. 2005a; Carter et al. 1993) for 125 °C, we see in Figure 4a that the current data on natural halite2 and 3 have got the upper limit by Wawersik et al. (Wawersik & Zeuch 1986) (unknown water content) and Ter Heege et al. (2005a) (wet), whereas Carter et al. (1993) (dry) gives the lower bounds. The data of synthetic sample halite1 show weaker behaviour and lie in approximation of Wawersik & Zeuch (1986)] and Ter Heege et al. (2005a).

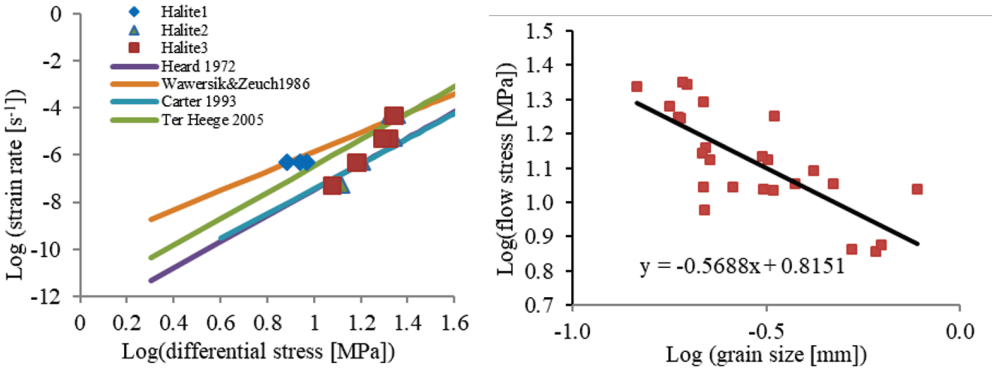

(a) (b)

Figure 4: a) Log-log plot of strain rate vs. differential stress, comparing the current results with the results of previous studies on wet and dry halite at 125 °C. (Heard 1972; Wawersik & Zeuch

1986; Carter et al. 1993; Ter Heege et al. 2005a), b) Log-log plot of differential stress vs. grain size for wet synthetic halite (Ter Heege et al. 2005b)

4.2 Composite flow law

Provided physical conditions (like pressure and temperature) are fixed, the microstructure of the sample may be expected to remain constant during stress relaxation with limited straining (Rutter & Mainprice 1978) while processes such as dynamic (syn-deformational) recrystallization and grain growth are likely to affect the microstructure during deformation that results in substantial increase in strain. The relaxation data show that the dependence of strain rate on stress approaches linearity at low stress and slow strain rate, which observation has been used above to suggest that grain size sensitive behaviour might play a role.

We thus consider if the flow behaviour of wet halite can be described by a composite flow equation of grain size insensitive (GSI) and grain size sensitive (GSS) behaviour

$$\dot{\varepsilon} = A^*\sigma^n + B^*\sigma d^{-p} \quad (3)$$

where $\dot{\varepsilon}$ is the strain rate, σ the differential stress, A^* and B^* are constants at a given temperature, n is the stress exponent, d is the grain size and p is the grain size exponent.

To evaluate Equation (3), we need to estimate what the grain size was during deformation of our halite samples. We do this by using a conventional piezometric relation, allowing predicting what the dynamically recrystallized grain size was at a certain stress value (De Bresser et al. 2001)

$$d = K\sigma^{-m} \quad (4)$$

where K and m are material and mechanism specific constants. This relationship between stress and recrystallized grain size is generally assumed to be independent of temperature, although that there is evidence that this assumption is not generally valid.

Ter Heege et al. (2005b) established a piezometric relation between the grain size d and differential stress σ by measuring the grain size of experimentally deformed synthetic halite

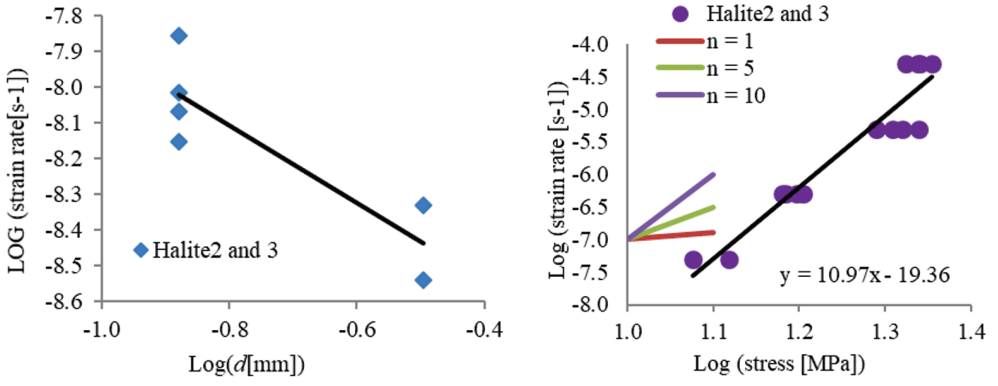

Figure 5: a) Strain rates picked from relaxation curves at fixed stress value (σ =6.3[MPa]) against the recrystallized grain size calculated using the piezometer relation of Eq. 5, b) Log-log plot for conventional power law ($\dot{\varepsilon} = \sigma^n$). The slope of the curve represents the stress exponent n-value. Three slopes lines corresponding to n = 1, 5 and 10 are also projected according to scale. The slope of halite2 and 3 combined data is very high (i.e. $n \sim 11$).

samples. The data by the authors are shown in the Figure 4b along with the best fit linear trend. The halite samples tested here (halite2 and 3) are natural salt samples, but we assume that

the same piezometer relation holds at current conditions of temperature and pressure; 125 °C and 50 MPa respectively.

Using the slope and intercept values of the best fit line in Figure 4b, we obtained values for *K* and *m* as 27.1 and 1.75 respectively, so the Equation (4) reduces to

$$d = 27.1\sigma^{-1.76} \quad (5)$$

The values of *d* represent the grain sizes at the end of the constant strain rate parts of the experiments, and hence, the grain sizes at the start of the relaxation parts. Assuming now that the microstructure remains constant during relaxation, these are the grain sizes applicable at the behaviour at $n \approx 1$. This allows us to estimate the *p*-value of Equation (3), in which stress is linearly dependent on strain rate. Taking logarithms and simplifying Equation (3), we get

$$log\dot{\varepsilon} = (logB^* + log\sigma) - plogd \quad (6)$$

or

$$log\dot{\varepsilon} = intercept - plogd \quad (7)$$

To keep the intercept part of this equation as a true constant, a fixed value of log stress (0.8) was selected (i.e. 6.3 MPa). For this fixed value of stress, log strain rate values were picked from the stress relaxation curves (Figs. 3(b-c)). Note that halite1 was not used in this analysis being different. The selected strain rate values are thus plotted against the calculated grain size *d* values in Figure 5a.

Regression analysis revealed a *p*-value of 1.1 (±0.3). This *p*-value supports the hypothesis that during stress relaxation, grain size sensitive (GSS) creep might play a role. It is well known that (GSS) solution-precipitation mechanisms may play an important role in the creep of fine-grained halite, creep (Spiers et al. 1990; Raj 1982; Schutjens 1991; Cox & Paterson 1991). According to these authors, a *p*-value of about 1 suggests, that the rate controlling step in the process will be dissolution or precipitation rather than diffusion. Accordingly, we infer that dissolution/precipitation-controlled pressure solution processes dominate the creep of wet halite at low stress and slower strain rate, at 125 °C.

Now using the intercept value of the best fit line in Figure 5a, the unknown constant B^* gets the value of 1.68×10^{-10} ($MPa^{-1}\ mm^{1.1}\ s^{-1}$), so the GSS creep equation becomes

$$\dot{\varepsilon}_{GSS} = 1.68 \times 10^{-10}\sigma d^{-1.1} \quad (8)$$

For the GSI part of Equation (3), we assume that conventional power law is applicable; plotting the steady points of halite2 and 3, against the deformation strain rates (Figure 5b), the values of *n* and A^* come out to be ~11 and 4.365×10^{-20} s^{-1} MPa^{-11}, so the GSI part can be written as

$$\dot{\varepsilon}_{GSI} = 4.365 \times 10^{-20}\sigma^{11} \quad (9)$$

The GSS flow law (Eq. 8) is based on the calculated grain size - strain rate data at σ = 6.3 MPa under the assumption that there is no influence of GSI flow at that condition. So, the GSS flow law (Eq. 8) is the right-handed end member of the composite description of Equation (3). Its trends for four different grain sizes are plotted in Figure 6a, where the trend for the steady state data (halite2 and 3) is included, as described by Equation (9). Equation (9), however, cannot simply be regarded as the left-hand (GSI) end member of the composite flow law (Eq. 3), since grain size sensitive behaviour might have influenced the steady state creep without realizing it. We thus took the data of halite2 and 3 from Table I and fitted them to Equation 3, using the established values for *n*, *p* and B^* and applied non-linear regression. This resulted in a value of 6.42×10^{-20} ($MPa^{-11}s^{-1}$) for A^*. The composite flow law (Eq. 3) now can be written

$$\dot{\varepsilon} = 6.42 \times 10^{-20}\sigma^{11} + 1.68 \times 10^{-10}\sigma d^{-1.1} \quad (10)$$

The trend lines in Figure 6b show that the influence of grain size is effective at lower stresses and strain rates. For higher stresses, these curves satisfy the steady state points, whereas on lower stress/strain rates, these trends satisfy the data picked from relaxation curves. So, the composite flow law gives a complete picture of the creep characteristics of natural wet halite

samples, in two regimes of GSI (n ~ 11) and GSS (n ~ 1) that gradually pass into each other on higher stress and faster strain rate side.

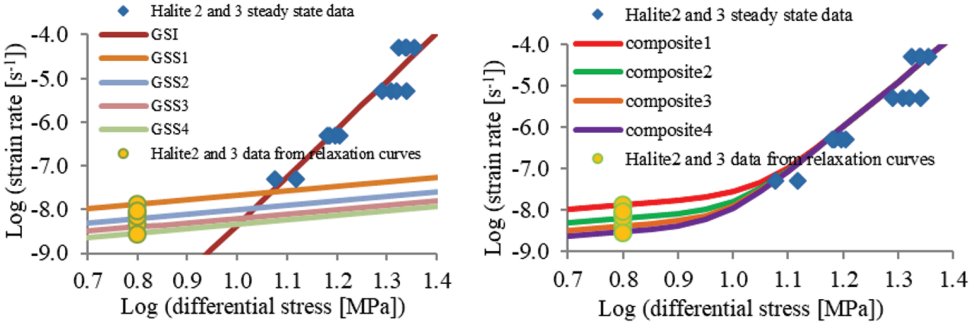

Figure 6. a) Log-log plot of strain rate and differential stress showing the predicted trends for GSS creep applying Eq. 8 for different grain sizes (GSS1, 2, 3 and 4 for d = 0.1, 0.2, 0.3 and 0.4 mm respectively), satisfying the lower stress and slower strain rate data. Note that higher grain sizes are lower in strain rates. The trend for GSI creep applying Eq. 9, satisfies the steady state values of constant deformation data, b) Log-log plot of strain rate and differential stress showing the predicted trends applying the composite creep Eq. 10, for a grain size of 0.1 mm (composite1), 0.2 mm (composite 2),0.3 mm (composite 3) and 0.4 mm (composite 4).

5. Conclusions

The main research question addressed in this study was if a transition can be observed, in wet polycrystalline halite, from creep behaviour governed by a (grain size insensitive) dislocation mechanisms to creep behaviour controlled by a (grain size sensitive) solution-precipitation mechanism, and if so, what the conditions of this transition are in terms of strain rate.

The experiments on the synthetic and natural halite samples at a confining pressure of 50 MPa and temperature of 125 °C revealed that at faster strain rates and higher stresses, dislocation creep (GSI) plays its role, which can be described by a conventional power law creep equation with n = 11. With such a high value, dislocation climb is unlikely to be rate controlling, but a dislocation glide mechanism should be considered. During the stress relaxation parts of the experiments, the n-value decreased to ~1 and a grain size sensitive creep mechanism, most probably pressure solution, becomes operative with the dissolution/precipitation step as rate controlling, as revealed by an analysis of the grain size exponent of creep (p ~ 1), using a flow equation of the type $\dot{\varepsilon} = B^{*}\sigma d^{-p}$.

The transition from (presumably) glide controlled dislocation creep with high power law n-value to grain size sensitive creep at n ~ 1, at 125 °C, occurs at a strain rate of about 10^{-9} s^{-1}. So, at slow strain rates ~10^{-9} s^{-1}, at a depth equivalent to an overburden/hydrostatic pressure of 50 MPa, grain size sensitive creep mechanism plays a more important role than dislocation mechanisms.

Acknowledgements

This work was supported through a scholarship for NM awarded by the Higher Education Commission of Pakistan and through additional sponsorship provided independently by AkzoNobel, Nedmag Industries and the Nuclear Research and Consultancy Group NRG. The authors thank Gert Kastelein, Peter van Krieken and Eimert de Graaff for technical support.

References

AUTEN T.A., DAVIS L.A. & GORDON R.B. 1973 Hydrostatic pressure and the mechanical properties of NaCl polycrystals. Philosophical Magazine, 28, 335-341.

CARTER N.L. & HANSEN F.D. 1983 Creep of rocksalt. Tectonophysics, 92(4), 275-333.

CARTER N.L., HORSEMAN S.T., RUSSELL J.E. & HANDIN J. 1993 Rheology of rocksalt. Journal of Structural Geology, 15 (9-10),1257-1271.

COX S.F.& PATERSON M.S. 1991 Experimental dissolution-precipitation creep in quartz aggregates at high temperatures. Geophysical Research Letters 18.8: 1401-1404.

DE BRESSER J.H.P., TER HEEGE J.H. & SPIERS C.J. 2001 Grain size reduction by dynamic recrystallization: can it result in major rheological weakening? International Journal of Earth Sciences, 90(1), 28-45.

DING J., CHESTER F.M. CHESTER J.S., X. SHEN & ARSON C. 2021 Coupled brittle and viscous micromechanisms produce semibrittle flow, grain-boundary sliding, and anelasticity in salt-rock."Journal of Geophysical Research: Solid Earth 126, no. 2.

FRANSSEN R.C. 1994 The rheology of synthetic rocksalt in uniaxial compression. Tectonophysics, 233(1), 1-40.

HEARD H.C. 1972 Steady-State Flow in Polycrystalline Halite at Pressure of 2 Kilo bars,"Flow and Fracture of Rocks, 191-209.

HEARD & RYERSON F.J. 1986 Effect of Cation Impurities on Steady-State Flow of Salt,"Mineral and Rock Deformation: Laboratory Studies: The Paterson Volume, 99-115.

JACKSON M.P.A. & TALBOT C.J. 1986 External shapes, strain rates, and dynamics of salt structures," Geological Society of America Bulletin 97.3: 305-323.

MUHAMMAD N. 2015 Deformation and transport processes in salt rocks: An experimental study exploring effects of pressure and stress relaxation. Utrecht Studies in Earth Sciences, 84, 1-275.

PEACH C.J. 1991 Influence of deformation on the fluid transport properties of salt rocks," Geologica Ultraiectina, 77, 1-238.

PEACH C.J., SPIERS C.J. & TRIMBY P.W. 2001 Effect of confining pressure on dilatation, recrystallization, and flow of rock salt at 150 °C. Journal of Geophysical Research: Solid Earth (1978–2012) 106.B7: 13315-13328.

POIRIER J.P. 1985 Creep of crystals: high-temperature deformation processes in metals, ceramics and minerals. Cambridge University Press.

RAJ R. 1982 Creep in polycrystalline aggregates by matter transport through a liquid phase," Journal of Geophysical Research: Solid Earth (1978–2012)87. B6: 4731-4739.

ROEDDER E. & BASSETT R.L. 1981 Problems in determination of the water content of rock-salt samples and its significance in nuclear-waste storage siting. Geology 9, no. 11: 525-530.

RUTTER E.H. & MAINPRICE D.H. 1978 "The effect of water on stress relaxation of faulted and unfaulted sandstone," Pure and Applied geophysics 116.4-5: 634-654.

SCHUTJENS P.M.T.M. 1991 Intergranular pressure solution in halite aggregates and quartz sands: an experimental investigation. Geologica Ultraiectina, 76, 1-233.

SENSENY P.E., HANSEN F.D., J.E. RUSSELL J.E. CARTER N.L. & HANDIN J.W. 1992 Mechanical behaviour of rock salt: phenomenology and micromechanisms", International journal of rock mechanics and mining sciences & geomechanics abstracts, vol. 29, no. 4, 363-378.

SKROTZKI W., FROMMEYER O. & HAASEN P. 1981 Plasticity of polycrystalline ionic solids. physica status solidi (a), 66 (1), 219-228.

SPIERS C.J., URAI J.L. LISTER G.S. BOLAND J.N. & ZWART H.J. 1986 The influence of fluid-rock interaction on the rheology of salt rock," Commission of the European Communities, Luxembourg.

SPIERS C.J., SCHUTJENS P.M.T.M., BRZESOWSKY R.H., PEACH C.J., LIEZENBERG J.L. & ZWART H.J. 1990 Experimental determination of constitutive parameters governing creep of rocksalt by pressure solution. Geological Society, London, Special Publications 54, 215-227.

TER HEEGE J.H., DE BRESSER J.H.P. & SPIERS C.J. 2005a Rheological behaviour of synthetic rocksalt: The interplay between water, dynamic recrystallization and deformation mechanisms. J. Struct. Geol. 27, 948-963.

TER HEEGE J.H., DE BRESSER J.H.P. & SPIERS C.J. 2005b Dynamic recrystallization of wet synthetic polycrystalline halite: dependence of grain size distribution on flow stress, temperature and strain," Tectonophysics 396.1: 35-57.

URAI J.L. 1983 Water assisted dynamic recrystallization and weakening in polycrystalline bischofite. Tectonophysics 96.1: 125-157.

URAI J.L., SPIERS C.J. ZWART H.J. & LISTER G.S. 1986 Weakening of rock salt by water during long-term creep," Nature; 324(6097): 554-7.

URAI J.L., C.J. SPIERS C.J. PEACH R.C.M.W. FRANSSEN & J.L. LIEZENBERG 1986 Deformation mechanisms operating in naturally deformed halite rocks as deduced from microstructural investigations," Geologie en Mijnbouw 66, no. 2: 165-176.

VAN EEKELEN H.A., HULSEBOS T. & URAI J.L. 1981 Creep of bischofite. The Mechanical Behavior of Salt: Proceedings of the First Conference Held at the Pennsylvania State University, University Park, Pennsylvania, Gulf Pub Co.

WAWERSIK W.R. & ZEUCH D.H. 1986 Modeling and mechanistic interpretation of creep of rock salt below 200 °C," Tectonophysics, 121(2), 125-152.

WEERTMAN J. 1957 Steady-State Creep of Crystals. J. Applied Physics, 28(10), 1185-1189.